GEOPHYSICS, VOL. 72, NO. 5 (SEPTEMBER-OCTOBER 2007); P. SM273–SM280, 12 FIGS., 2 TABLES.
10.1190/1.2759479

Decoupling of seismic reflectors and stratigraphic timelines: A modeling study of Tertiary strata from Svalbard

Ståle Johansen[1], Espen Granberg[2], Donatella Mellere[3], Børge Arntsen[4], and Torben Olsen[5]

ABSTRACT

In sequence stratigraphic interpretations, the key premise is that stratal surfaces effectively represent geologic timelines. When applied to seismic sections, the fundamental assumption is that primary reflections generally mimic stratigraphic timelines. The main objective of this study was to test how well key reflectors in a seismic section couple to timelines. To achieve the high level of ground control needed for such testing, we combined photogrammetry and traditional sedimentologic fieldwork to optimize the geologic model. We relied further on petrophysical analysis to derive a numerical model suitable for the simulation of seismic data. In spite of laterally discontinuous vertical-impedance contrasts (VICs), false seismic continuity was created, and we observed frequent decoupling of seismic reflectors and stratigraphic timelines. These observations demonstrate how the low-frequency seismic method fails to image normal complexity in a stratigraphic unit. A seismic correlation test showed that the interpreters made numerous mistakes and that such mistakes are very difficult to avoid. The failure of a fundamental assumption, as illustrated here, creates serious problems for the sequence stratigraphic concept when applied to detailed correlation analysis on seismic sections.

INTRODUCTION

Seismic data are the most important data type used for subsurface studies. Based on seismic interpretation results, very expensive wells are drilled. A typical average success rate for exploration wells is 1:4. A large portion of failures in subsurface mapping is obviously a result of incorrect seismic interpretations.

In sequence stratigraphic interpretations, the key premise is that stratal bedding surfaces effectively represent geologic timelines (Vail et al., 1977; van Wagoner et al., 1990). However, seismic sections show the response of the earth to seismic waves, and the position of geologic bedding is only one of several factors that affect this response. Stratigraphic conclusions from seismic data depend on the data being sufficiently free of noise so that the seismic response is predominantly that of the sediments. Thus, good recording and processing are essential (Sheriff, 1977). But first and foremost, the results depend on how well the sequence stratigraphic concept itself works when applied to seismic sections. The fundamental assumption is that primary reflections generally mimic stratal surfaces (timelines) within a stratigraphic section (Mitchum et al., 1977; Vail and Mitchum, 1977; Bally, 1987). The main objective of this study is to test how well key reflections in the actual seismic section represent stratigraphic timelines.

Forward seismic modeling allows testing of the relationship between geology and seismic response, and it is potentially very well suited for testing interpretation methodology. To get the best possible result, synthetic seismic data were simulated based on a geologic model from well-exposed and well-documented outcrops in Van Keulenfjorden, Svalbard, in the Norwegian Arctic. These outcrops are excellent for studies of lateral facies relationships; timelines can be traced from gravity-flow sand deposits on the basin floor up into coeval shoreface and floodplain fines. To make the simulated seismic data as realistic as possible, we combined geologic and geophysics methods in an integrated outcrop study.

Basically, we found that the low-resolution seismic method cannot image normal complexity in a stratigraphic unit. A seismic interpretation test showed that the interpreters made numerous correlation mistakes and that such mistakes are very difficult to avoid. If this result is also valid for real seismic sections, it creates serious prob-

Manuscript received by the Editor December 1, 2006; revised manuscript received May 3, 2007; published online August 23, 2007.
[1]EMGS, Stiklestadveien, Trondheim, Norway. E-mail: sj@emgs.com.
[2]Statoil, Harstad, Norway. E-mail: esg@statoil.com.
[3]Norske Shell, Tanager, Norway. E-mail: donatella.mellere@shell.com.
[4]Statoil Research Centre, Postuttak, Trondheim, Norway. E-mail: barn@statoil.no.
[5]Statoil, Stavanger, Norway. E-mail: tool@statoil.com.

lems for the sequence stratigraphic concept when applied to seismic sections for detailed correlation purposes.

INTEGRATED OUTCROP STUDY

Reliable ground control normally is hard to achieve with traditional subsurface models because of insufficient lateral well density. A better approach is to perform forward modeling on models from well-exposed and well-documented outcrops (Biddle et al., 1992; Johansen et al., 1994). The continuous outcrops of Eocene floodplain to basin-floor deposits (Figure 1) in Van Keulenfjorden are excellent for such studies. Timelines can be traced from gravity-flow sand deposits in the basin floor up into coeval shoreface and floodplain fines.

To make the geomodels as realistic as possible, we used photogrammetry combined with traditional sedimentological fieldwork. For modeling, we used a 2D elastic wave propagation modeling package that simulates a seismic section by successively computing the different shot records. In summary, the steps in the integrated outcrop study comprise (1) geological fieldwork, (2) photogrammetry, (3) petrophysical analysis, (4) seismic modeling, (5) seismic processing, and (6) seismic interpretation.

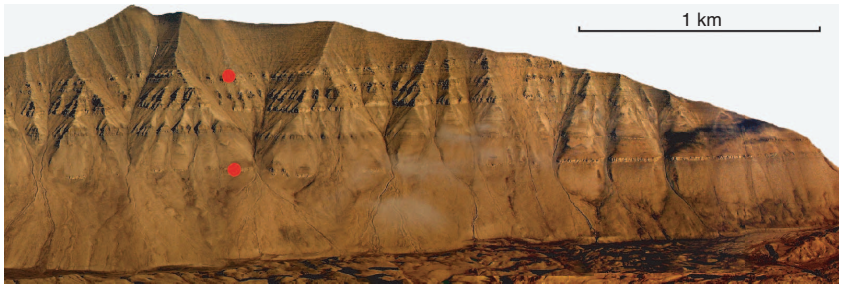

Figure 1. Photomosaic of the Tertiary exposures in Van Keulenfjorden. The lowermost sandstone (yellow) in the middle right of the picture, marked with the lower red dot, is the lowermost sandstone in Figure 3a. The top of the mountain can be used as reference when comparing with Figure 3a. Note that the photo is taken from the ground, so the geometry is not correct as seen in the picture. The vertical distance between the red dots is 350 m.

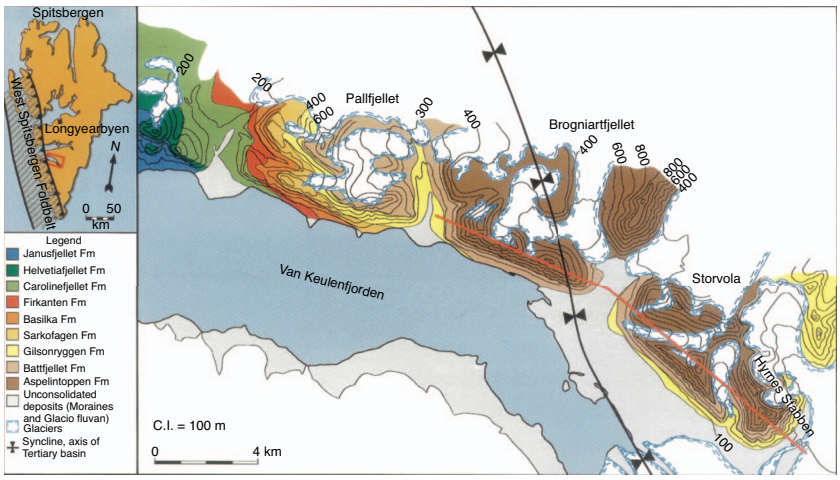

Figure 2. Locality map of the Van Keulenfjorden exposures on Spitsbergen, Svalbard. The Brogniartfjellet, Storvola, and Hyrnestabben outcrops consist of clinoforms reflecting Eocene infilling of the Central Basin. The red line shows the locations of the profiles in Figure 3.

Geologic setting, fieldwork, and photogrammetry

The onshore Tertiary basins of Svalbard are all situated on the main island of Spitsbergen (Figure 2), where they line up along a mobile belt that deformed the western margin of this island during Paleogene time. The late Paleocene-Eocene Central Basin was a relatively small foreland basin formed in front of the developing fold-and-thrust belt (Harland, 1965, 1969; Lowell, 1972). (For details on the Tertiary development, see also Kellog, 1975; Myhre et al., 1982; Spencer et al., 1984; and Steel et al., 1985.) The latest Paleocene–early Eocene infilling of the Central Basin progressed from west to east and left a spectacular record of large-scale (hundreds of meters) shallow to deepwater clinoforms. These are now exposed along the mountainsides, reflecting the overall progradation from coastal plain to delta/barrier shoreline via a ramp slope to a basin-floor sedimentary system (Helland-Hansen, 1990, 1992).

In Van Keulenfjorden, a detailed stratigraphic profile encompassing the mountainsides of Brogniartfjellet, Storvola, and Hyrnestabben was investigated (Figure 2). A photogrammetric approach (Dueholm, 1990, 1992; Dueholm and Olsen, 1993) was selected to ensure that the resultant 2D cross section is free of artificial thickness variations and allows good control of lateral continuity of lithofacies and stratigraphic timelines.

The architecture of the mountainsides appears rather simple when seen from a distance. A lower, poorly exposed marine shale unit (Gilsonryggen Formation) is overlain by a sandstone unit of shoreface origin (Battfjellet Formation). The entire overlying part of the exposures consists of moderate to poorly exposed thin, fluvial sandstone lenses in a matrix of floodplain fines (Aspelintoppen Formation; Figure 2). Photogrammetric mapping, however, reveals a significant complexity in all three parts, particularly in the middle sandstone bench (Figure 3).

In addition to photogrammetric mapping, 13 vertical sedimentological sections were measured. In this way, the key lithologies and facies associations were established and a sequence stratigraphic framework was constructed. Further stratigraphic details of the Van Keulenfjorden outcrops are discussed in Steel et al. (2000), Mellere et al. (2003), and Steel and Olsen (2002).

Petrophysical analysis and impedance model

Accurate estimation of velocity and density distribution was the most difficult step in this integrated outcrop study. Because these parameters vary in two dimensions within the model, any values assigned to a given layer must be considered an approximation. Implicit in this process is the assumption that acoustic impedance is related directly to lithology. Other factors such as pore-fluid composition and pore pressure also have effects on the acoustic impedance, but such factors are not fully taken into account in this study. However, the values used are representative for

the individual facies, and the resulting impedance contrasts are comparable to contrasts seen in well logs from similar geologic settings.

To constrain the velocity and density variations from the outcrops, we used laboratory measurements of rock samples and compared these results with logs from one well. P-wave velocity, S-wave velocity, and densities were measured on 39 samples. A representative suite of lithologies was sampled from the measured sections. Petrophysical properties were measured directly from hand specimens at ambient surface pressure and temperature. Each sample was first measured by a P-wave recorder and then by an S-wave recorder (all by a 500-kHz frequency pulse). Finally, bulk densities were measured by an Archimedean technique. The results of the velocity and density measurements are shown in Figure 4.

Key facies associations from the geologic model are listed in Table 1. The coastal-plain facies association is divided in two: a coastal-plain shale facies and a fluvial sandstone facies. For the shaly lithofacies, we have no reliable petrophysical outcrop measurements because of cracked samples. Interval velocities for the shaly lithofacies were gathered from an exploration well (Ishøgda-1) approximately 35 km north of Van Keulenfjorden. Here, sonic velocities for the shales are approximately 25% lower compared to the surrounding sandstones. For the rest of the lithofacies, mean values were computed from the measured samples (Table 1). The average density values show little variation. Because the seismic velocities are the dominating factor for the impedance values, we have chosen the density for all sandy lithofacies to be 2.6 g/cm^3. For the shaly lithofacies, we used 2.5 g/cm^3.

Vertical-impedance contrasts (VICs) are quite well controlled, while lateral changes in velocity are less well constrained. This has to some extent been accounted for in the model (Figure 5), but lateral variations are more difficult to sample correctly in the field. The present-day mountain topography was removed from the impedance model and, to make as realistic a synthetic seismic section as possible, the Van Keulenfjorden strata were "buried" under 1100–1400 m of overburden rock. This was done by using P-wave velocities, S-wave velocities, and densities from Tertiary strata drilled by a North Sea well. All layers in the overburden are continuous. To simulate marine acquisition, a water layer was added on top of the model (Figure 6).

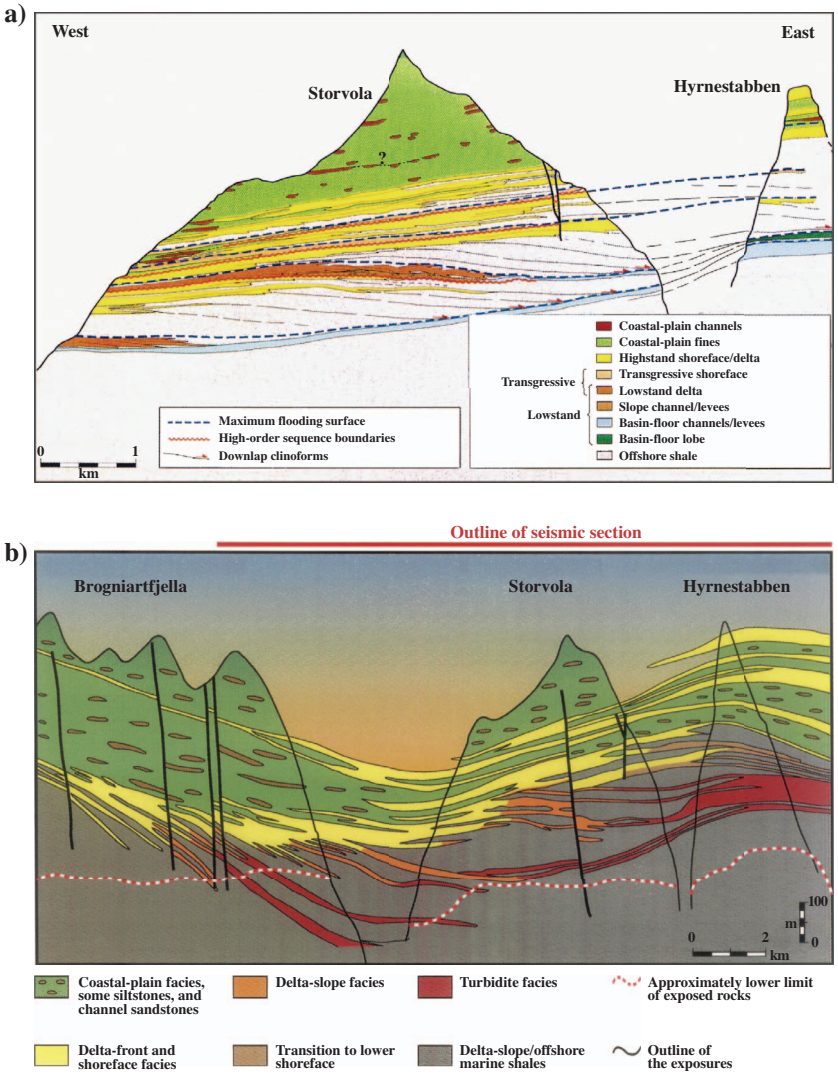

Figure 3. (a) Stratigraphic and lithologic model of the Storvola and Hyrnestabben outcrops, Van Keulenfjord. Note: 4× vertical exaggeration. See Figure 2 for location of profile. (b) Schematic lithologic model of the Brogniartfjellet, Storvola, and Hyrnestabben outcrops, Van Keulenfjord. The corresponding rock properties are given in Table 1. See Figure 2 for location of profile.

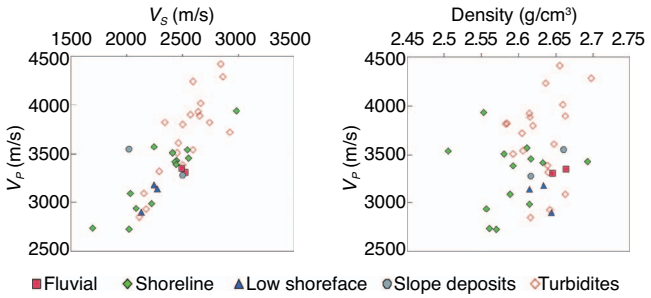

Figure 4. (a) P-wave velocities versus S-wave velocities obtained from laboratory measurements of rock samples from outcrops in Van Keulenfjorden. Samples were grouped according to depositional facies, and mean values were calculated for each facies (see Table 1). Two additional facies types were used in the modeling: coastal-plain fines and offshore shales. The modeling parameters for these facies were taken from an exploration well located 35 km north of the exposures (see small map in Figure 2). (b) P-wave velocities versus densities obtained from laboratory measurements of rock samples from outcrops in Van Keulenfjorden. Densities used in this study are given in Table 1.

Seismic modeling

We generated two types of modeled data. The reflectivity section derived from the impedance model was first convolved with a minimum-phase Ricker wavelet. The resulting seismic section assumes vertical incidence to surfaces (image ray modeling) and simulates a migrated seismic line. The other seismic model was generated by a 2D elastic-wave propagation modeler that uses a high-order space and a second-order time finite-difference scheme (Mittet and Renlie, 1996).

Causes of the three main sources of errors in finite-difference modeling are (1) the determination of spatial and temporal derivatives, (2) the finite size of the model (edge reflections), and (3) the general implementation of the scheme. To control the errors related to spatial derivatives, we used optimized high-order difference operators as proposed by Holberg (1987). The absorbing boundary conditions used to minimize edge effects were implemented as in Cerjan et al. (1985), and the general implementation of the medium parameters was done as in Mittet and Renlie (1996).

The input to the 2D modeler consists of grids of P-wave velocity, S-wave velocity, and density. The grid size is 2×2 m. The average frequency content in the target area is approximately 30 Hz. A standard 2D marine acquisition was simulated with recording parameters given in Table 2. To imitate industry workflow, the processing was done by a provider outside the project; the correct velocities were known to the processor. The selected processing sequence as such is not evaluated in this paper. Vien et al. (1997) discuss aspects of processing this data set in detail, but their processing sequence differs from the one used in this study.

Table 1. P-wave velocities, S-wave velocities, and densities selected for use in the reservoir model.

Lithology/facies association	P-velocity	S-velocity	Density	V_P/V_S	Basis for choosing values
Turbidite facies	3.69	2.53	2.6	1.458	Average values within this type of facies (from petrophysical measurements)
Delta-slope facies	3.42	2.26	2.6	1.513	Average values within this type of facies (from petrophysical measurements)
Fluvial sandstones (within the coastal-plain Aspelintop pen Formation)	3.33	2.51	2.6	1.327	Average values within this type of facies (from petrophysical measurements)
Shoreface/delta-front facies	3.29	2.31	2.6	1.424	Average values within this type of facies (from petrophysical measurements)
Lower shoreface hetereoliths (transition to lower shoreface)	3.07	2.21	2.6	1.389	Average values within this type of facies (from petrophysical measurements)
Delta-front/ offshore marine shales	2.77	1.9	2.5	1.458	P- and S-velocities are 75% of the value used for the turbidite sandstones. This agrees with the Ishøgda well.
Coastal-plain shales and siltstones (Aspelintoppen Formation)	2.47	1.73	2.5	1.428	P- and S-velocities are 75% of the value used for the turbidite sandstones. This agrees with the Ishøgda well.
Seawater	1.50	0	1		

OBSERVATIONS, INTERPRETATION, AND DISCUSSION

In interpreting the modeled seismic data, we focus on how well the correlation of key reflections represents timelines in the geologic model. The quality of reservoir models is highly dependent on how well this concept works in practice. When the impedance contrast is laterally discontinuous along the inferred timeline, the correlation can fail, especially considering the limited resolution of the seismic images.

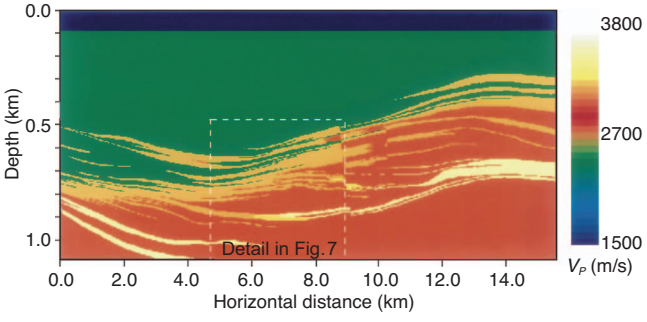

Figure 5. P-wave velocity model of Brogniartfjellet, Storvola, and Hyrnestabben, Van Keulenfjorden. See Figure 3 for comparison with stratigraphic and lithologic models and Figure 2 for location of the profile. Because the density variations are minor, this section also illustrates the impedance variations very well.

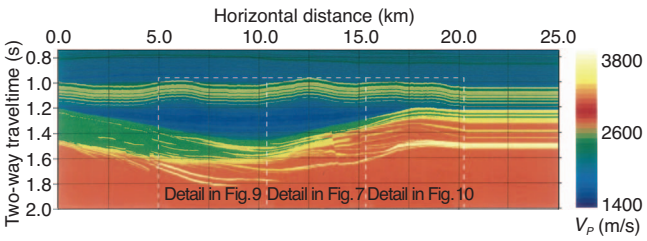

Figure 6. P-wave velocity model of Brogniartfjellet, Storvola, and Hyrnestabben combined with a constructed overburden model. The lower part of the model is an extended version of the model in Figure 5. Velocity distribution in the overburden is representative for Tertiary strata in the northern North Sea. See Figure 3 for comparison with geologic models and Figure 2 for location of profile. Because the density variations are minor, this section also illustrates the impedance variations very well.

Decoupling of timelines and reflectors

The simple seismic reflectivity model is included to illustrate how primary reflections interfere with and destroy the correlation of timelines. Figure 7a shows the velocity model that corresponds to the convolved results in Figure 7b. The velocity model is characterized by significant lateral discontinuity of VICs. From a purely sequence-stratigraphic perspective, it is possible to trace a large number of timelines through these facies associations, as shown in Figure 3a. These correlations are not based on VIC but on other stratigraphic criteria observed in the outcrops. However, in spite of VIC discontinuity, the low-frequency content creates false continuity and decouples stratigraphic timelines and seismic reflectors.

Artificial continuity is created, especially along reflectors A, B, and D (Figure 7b). The thin sandstones (yellow) pinching out into the shale (green) are seismically smeared and appear as the continuous reflector B. This reflection now defines the approximate base of a prograding sandstone unit and is, as such, not a stratigraphic timeline. Reflector B corresponds to a stratigraphic timeline at position 2 (Figure 7a), but this timeline decouples and continues toward the left just below the circle at position 7. It is very likely that such phenomena occur also on real seismic sections where sands pinch out into homogeneous shales.

Further, the continuous reflector A corresponds to boundary 4 in the right portion of the model, but this boundary is not continuous throughout the section. Again, the reflections merge and create a reflection pattern where the seismic reflectors are decoupled from the timelines. In addition, the termination at C is created in a similar way by interference of reflections from thin sandstone beds dipping at low angles.

Overburden model and correlation test

To obtain a more realistic seismic image, the Van Keulenfjorden model was buried under a stratified sedimentary overburden (Figure 6). The data look realistic, and the new seismic section (Figures 7c and 8) is dramatically changed from the simpler image discussed earlier. From Figure 7c, it is clear that the new seismic image is much more complex than the simple reflectivity section. New reflection patterns and terminations are created (H, I), and termination C is lost; it should have appeared at J.

Reflector decoupling is common throughout this seismic section. This creates problems for the interpreters because the fundamental assumption is that primary reflections should mimic timelines. Especially in the middle (Figure 7c) and left (Figure 9) portions of the section, it is very difficult for interpreters to identify the decoupling because the false events here are parallel or subparallel to primary reflectors.

In the eastern portion of the section (Figure 10), it is possible to identify the thicker deepwater sand accumulation by a combination of downlap and mounding. Here, at first glance, most reflectors seem to correspond to real stratal surfaces. However, false events and arti-

Table 2. Seismic acquisition parameters.

Parameter	Amount
Source depth	10 m
Shot interval	25 m
Maximum frequency content	80 Hz
Cable depth	10 m
Near offset	0 m
Far offset	2000 m
Group interval	12.5 m
Record length	3000 ms

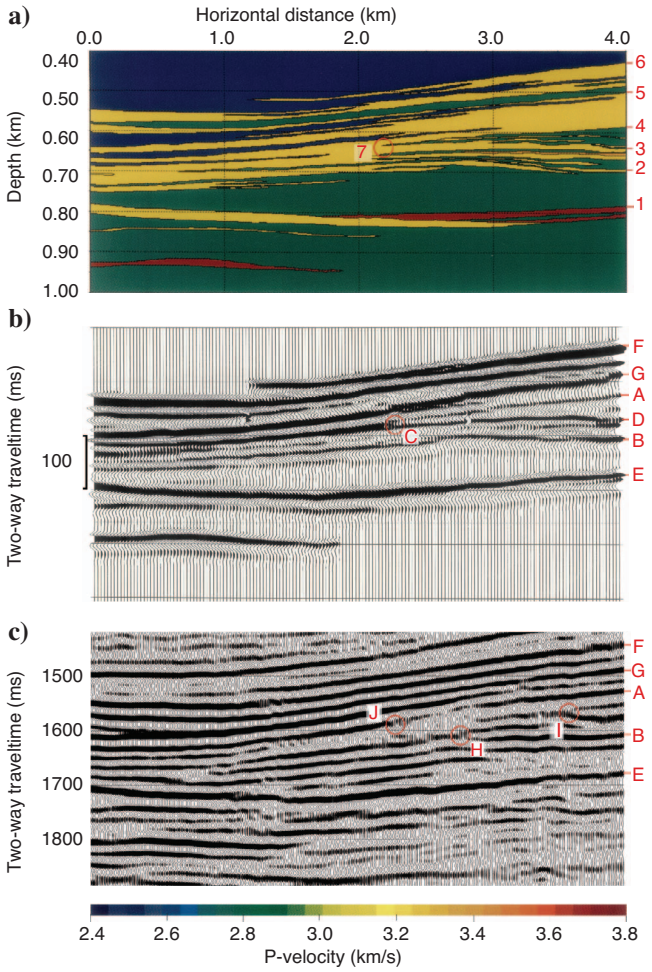

Figure 7. (a) Detail from the middle part of the P-wave velocity model in Figure 5. (b) Synthetic seismic section (30 Hz) of this velocity model. The reflectivity section derived from the impedance model was convolved by a minimum-phase Ricker wavelet. Because the resulting seismic section assumes vertical incidence to surfaces (image ray modeling), the section simulates a migrated seismic line. (c) Synthetic seismic section (finite-difference modeling algorithm) of the same velocity model. See text for detailed explanations.

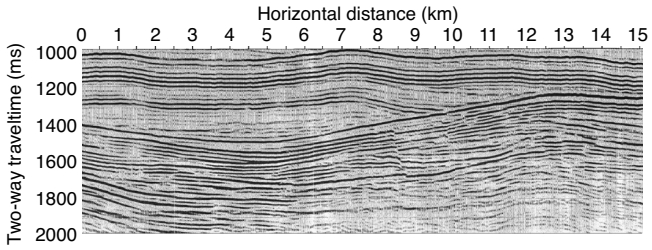

Figure 8. Synthetic seismic section (finite-difference modeling algorithm) of the model shown in Figure 6.

ficial continuity also occur in this part of the section. A clear indication of this is the presence of reflections below the lowest interface of the model.

A good way to check whether the timeline concept is valid is to perform a controlled interpretation test. The blue lines in Figure 11a show correct timelines from the geologic model. The red lines in Figure 11b are the result from the interpretation test. The interpretation was done by an experienced exploration seismologist outside the project. The same data set has also been used for training, and more than 50 seismic interpreters and close to 200 geology and geophysics students have interpreted the section. Most interpreters established the general geologic pattern in a reasonably good way, and the most experienced interpreters were able to deduce a depositional history from the data. However, all of the interpreters had serious problems with the detailed correlations. Figure 11b is representative of most of the interpretations performed on this data set. All interpreters had general background information about the geologic setting of the area.

The interpretation started from well 1 by picking high-amplitude continuous reflections. When reflectors split and it was doubtful which reflector should be followed, this point was marked with a circle. Across faults, however, the correct correlations were given to the interpreter. This was done to avoid uncertainty on how correlations across faults affected the result. The arrow direction (up/down) shows the actual choice the interpreter made. Question marks indicate general uncertainty in the correlation, e.g., as a result of weak amplitude or low continuity. For better visualization and easy comparison, the results were put together in the well correlation panel in Figure 12.

The two sets of timelines frequently cross each other, and many of the correlations are therefore wrong. This is not surprising, based on the earlier discussion where we saw how VIC discontinuities were camouflaged and how artificial continuity created new and false reflections that were easily interpreted as timelines. In the seismic sec-

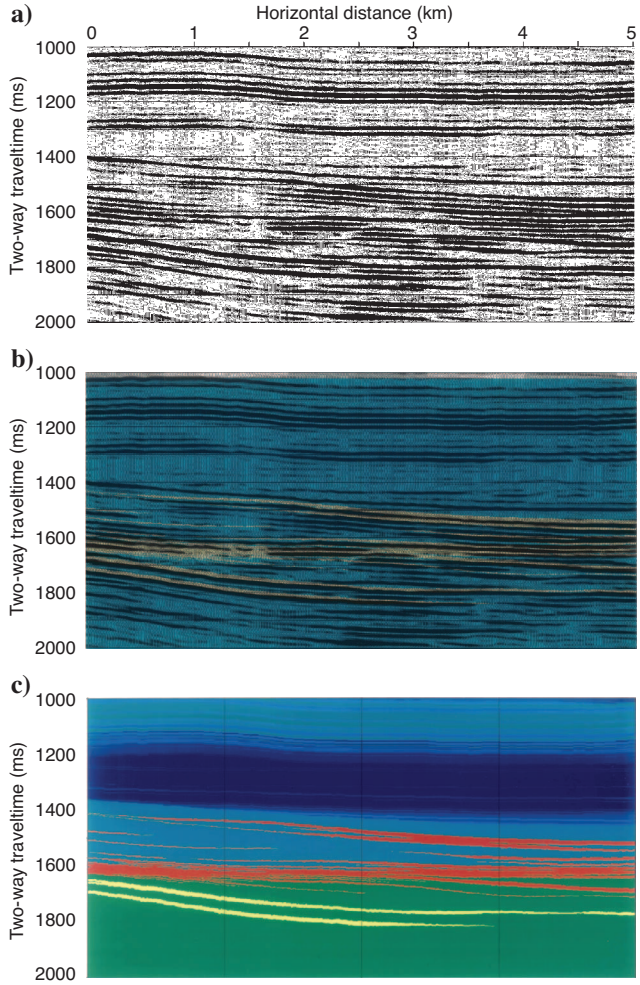

Figure 9. Synthetic seismic section (finite-difference modeling algorithm) of (a) the western portion of Figure 6 and (b) the western portion of Figure 6 combined with the P-wave velocity model. The color scale for the velocity model is compressed to distinguish sandy facies (yellow) from shales (blue). (c) Detailed P-wave velocity model of the western part of the Van Keulenfjorden outcrops. The sandy facies are red and yellow; the shaly facies are green and blue.

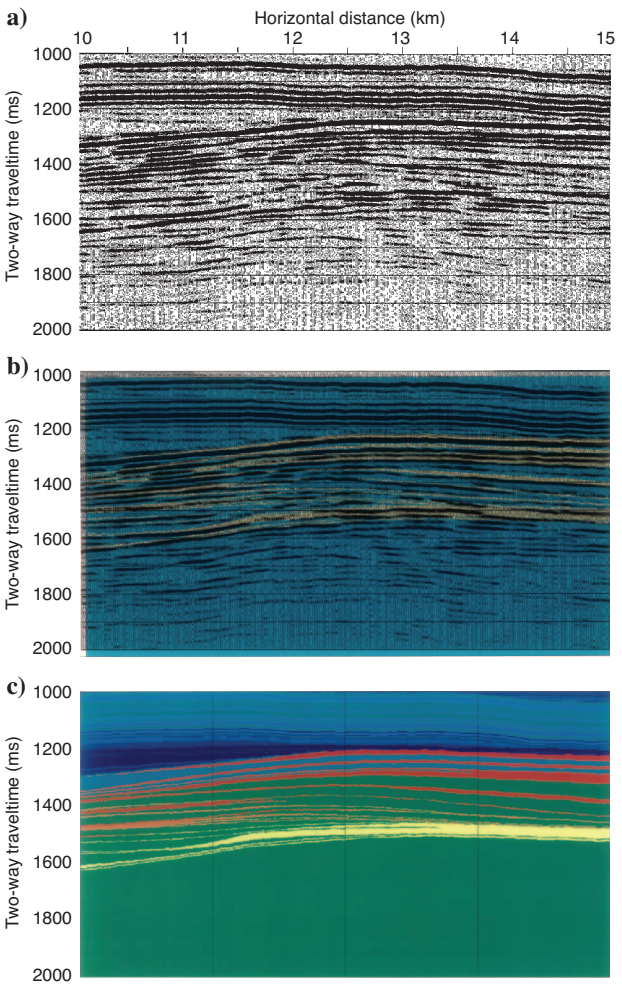

Figure 10. Synthetic seismic sections (finite-difference modeling algorithm) of (a) the eastern portion of Figure 6 and (b) the eastern portion of Figure 6 combined with the P-wave velocity model. The color scale for the velocity model is compressed to distinguish sandy facies (yellow) from shales (blue). (c) Detailed P-wave velocity model of the eastern part of the Van Keulenfjorden outcrops. The sandy facies are red and yellow; the shaly facies are green and blue.

tion discussed here, normal industry processing was performed, and the correct velocity model was given to the processing team. It is therefore fair to assume that this section is of at least average industry standard.

In summary, the data set failed to pass the correlation test. This potentially could create serious problems for the sequence stratigraphic concept when applied to seismic sections for detailed correlation purposes. The reason for this is that the key premise that seismic reflections should mimic stratal surfaces (timelines) is not fulfilled. When evaluating this statement, one must keep in mind that this analysis is based on simulated seismic data, and we realize that our conclusions are not better than the quality of the simulated data. However, the fundamentals of seismic-wave propagation are well understood, and the procedure used to construct the synthetic seismic data was very realistic. For these reasons, we suggest that our conclusions are also valid for real seismic data.

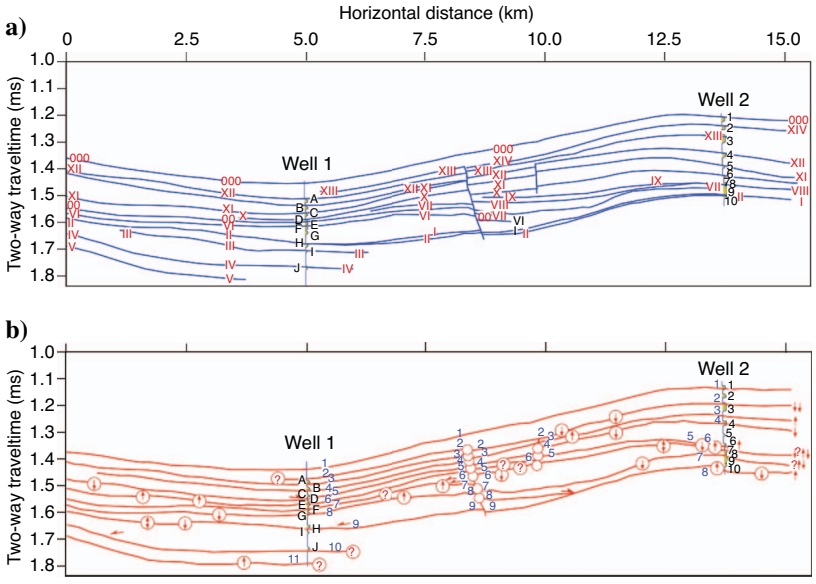

Figure 11. (a) Line drawing of correct timelines selected from the velocity model in Figure 6. (b) Line drawing from the correlation test. Numbers, letters, and arrows are used for easy reference to Figure 12. A circle indicates a choice, and the arrow shows the alternative direction for the correlation. A question mark means the correlation is uncertain because of poor reflector continuity. An open circle shows a correlation across a fault (see text).

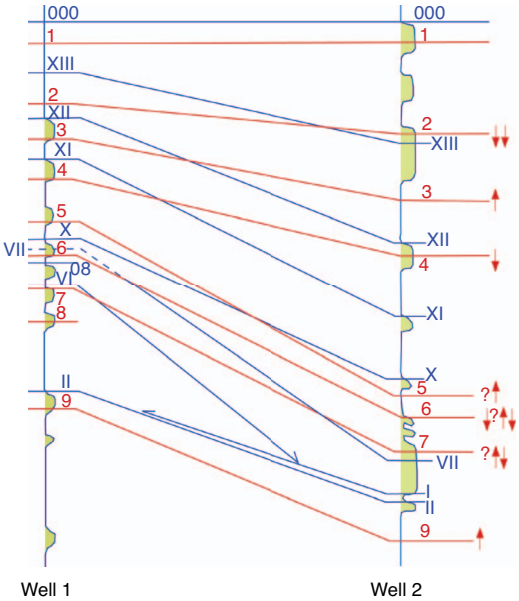

Figure 12. Simplified version of the two interpretations shown in Figure 11. An arrow shows the alternative direction for a correlation. A question mark means the correlation is uncertain because of poor reflector continuity.

CONCLUSIONS

Integrated outcrop studies, including geologic and geophysical elements, are a powerful tool for controlled studies of interpretation methodology. Photogrammetry or similar techniques must be used to obtain the accuracy required for such studies. To produce a realistic seismic section, overburden must be included, advance modeling must be performed, and a normal processing sequence must be applied to the data. However, it is also very useful to include a simple reflectivity section to understand the theoretical potential in the data.

In spite of VIC discontinuity, false seismic continuity was created, and frequent decoupling of seismic reflectors and stratigraphic timelines occurred. The reason for this is that the limited resolution of the seismic method cannot image normal complexity in a stratigraphic unit. To improve resolution significantly, unrealistically high frequencies would have to be recorded. The correlation test showed that although the interpreters made numerous correlation mistakes at the reservoir level, the resulting regional geologic model derived from the seismic section looked realistic. This indicates that such mistakes are very difficult to avoid. The failure of a fundamental assumption, as illustrated here, creates serious problems for the sequence stratigraphic concept when applied to detailed correlation analysis on seismic sections.

ACKNOWLEDGMENTS

We thank Statoil for permission to publish this paper. We also thank Andrew Morton, Rune Mittet, Stephen Johnson, Hans Amundsen, Stig Arne Karlsen, Anwar Hossain Bhuiyan, Trine Beate Karlsen, and Marit Raak Pettersen for valuable help and critiques. We thank our reviewers, especially Clement Kostov, who gave very valuable comments and suggestions that significantly improved the manuscript.

REFERENCES

Bally, A. W., 1987, Atlas of seismic stratigraphy: AAPG.

Biddle, K. T., W. Schlager, K. W. Rudolph, and T. L. Bush, 1992, Seismic model of a progradational carbonate platform, Pico di Vallandro, the Dolomites, northern Italy: AAPG Bulletin, **50**, 14–30.

Cerjan, C., D. Kosloff, R. Kosloff, and M. Reshef, 1985, A nonreflecting boundary condition for discrete acoustic and elastic wave equations: Geophysics, **50**, 705–708.

Dueholm, K. S., 1990, Multi-model stereo restitution: Photogrammetric Engineering and Remote Sensing, **56**, 239–242.

———, 1992, Geologic photogrammetry using standard small-frame cameras: Grønlands Geologiske Undersøkelse, **156**, 7–17.
Dueholm, K. S., and T. Olsen, 1993, Reservoir analog studies using multimodel photogrammetry: A new tool for the petroleum industry: AAPG Bulletin, **77**, 2023–2031.
Harland, W. B., 1965, The tectonic evolution of the Arctic-North Atlantic Region: Philosophical Transactions of the Royal Society of London, Series B, **258**, 59–75.
———, 1969, Contribution of Spitsbergen to understanding of tectonic evolution of the North Atlantic region, *in* M. Kay, ed., North Atlantic geology and continental drift: AAPG Memoir 12, 817–851.
Helland-Hansen, W., 1990, Sedimentation in a Paleogene foreland basin, Spitsbergen: AAPG Bulletin, **74**, 260–272.
———, 1992, Geometry and facies of Tertiary clinothems, Spitsbergen: Sedimentology, **39**, 1013–1029.
Holberg, O., 1987, Computational aspects of the choice of operator and sampling interval for numerical differentiation in large-scale simulation of wave phenomena: Geophysical Prospecting, **35**, 629–655.
Johansen, S. E., S. Kibsgaard, A. Andresen, T. Henningsen, and J. R. Granli, 1994, Seismic modeling of a strongly emergent thrust front, West Spitsbergen fold belt, Svalbard: AAPG Bulletin, 1018–1027.
Kellog, H. E., 1975, Tertiary stratigraphy and tectonism in Svalbard and continental drift: AAPG Bulletin, **59**, 465–485.
Lowell, J. D., 1972, Spitsbergen Tertiary orogenic belt and the Spitsbergen fracture zone: Geological Society of America Bulletin, **83**, 3091–3102.
Mellere, D., A. Breda, and R. Steel, 2003, Fluvially incised shelf-edge deltas and linkage to upper-slope channels (Central Tertiary Basin in Spitsbergen), *in* H. Roberts et al., eds., Global significance and future exploration potential: GCS-SEPM Special Publication, 231–266.
Mitchum, R. M., P. R. Vail, and S. Thompson, 1977, Seismic stratigraphy and global changes of sea level, Part 2: The depositional sequence as a basic for stratigraphic analysis, *in* C. E. Payton, ed., Seismic stratigraphy — Applications to hydrocarbon exploration: AAPG Memoir 26, 53–62.
Mittet, R., and R. Renlie, 1996, High-order finite-difference modeling of multipole logging in formations with anisotropic attenuation and elasticity: Geophysics, **61**, 21–33.
Myhre, A. M., O. Eldholm, and E. Sundvor, 1982, The margin between Senja and Spitsbergen fracture zones: Implications from plate tectonics: Tectonophysics, **89**, 33–50.
Sheriff, R. E., 1977, Limitations on resolution of seismic reflections and geologic detail derivable from them, *in* C. E. Payton, ed., Seismic stratigraphy — Applications to hydrocarbon exploration: AAPG Memoir 26, 3–14.
Spencer, A. M., P. C. Home, and L. T. Berglund, 1984, Tertiary structural development of the western Barents Shelf, Troms to Svalbard, *in* A. M. Spencer, ed., Petroleum geology of the North European Margin: Norwegian Petroleum Society, 199–209.
Steel, R., J. Gjelberg, W. Helland-Hansen, K. Kleinspehn, A. Nøttvedt, and M. R. Larsen, 1985, The Tertiary strike-slip basins and orogenic belt of Spitsbergen, *in* K. T. Biddle and N. Christie-Buck, eds., Strike-slip deformation, basins formation and sedimentation: Society of Economic Paleontologists Mineralogists Special Publication 37, 339–358.
Steel, R., D. Mellere, P. Plink, J. Crabaugh, J. Deibert, and M. Schellpeper, 2000, Deltas versus rivers on the shelf edge: Their relative contributions to the growth of shelf-margins and basin-floor fans (Barremian and Eocene, Spitzbergen): GCS-SEPM Special Publication 28, 981–1009.
Steel, R. J., and T. Olsen, 2002, Clinoforms, clinoform trajectories and deep-water sands, *in* J. M. Armentrout and N. C. Rosen, eds., Sequence stratigraphic models for exploration and production: Evolving methodology, emerging models and application histories: GCS-SEPM Special Publication, 367–381.
Vail, P. R., and R. M. Mitchum, Jr., 1977, Seismic stratigraphy and global changes of sea level, Part 1: Overview, *in* C. E. Payton, ed., Seismic stratigraphy — Applications to hydrocarbon exploration: AAPG Memoir 26, 51–52.
Vail, P. R., R. M. Mitchum, Jr., R. G. Todd, J. M. Widmier, S. Thomson III, L. B. Sangree, J. N. Bubb, and W. G. Hatlelid, 1977, Seismic stratigraphy and global changes of sea-level, *in* C. E. Payton, ed., Seismic stratigraphy — Applications to hydrocarbon exploration: AAPG Memoir 26, 51–212.
Van Wagoner, I. C., K. M. Campion, and V. D. Rahmanian, 1990, Siliciclastic sequence stratigraphy in well logs, core, and outcrops: Concepts for high-resolution correlation of time and facies: AAPG.
Vien, P. T., E. Tjåland, B. Arntsen, and S. Johansen, 1997, Optimum seismic processing of modeled outcrop data from Van Keulenfjord, Svalbard: 67th Annual International Meeting, SEG, Expanded Abstracts, 1395–1398.